New Results on Microwave and Terahertz Detection Using Metallic Single-Walled Carbon Nanotubes

Sigfrid Yngvesson, Kan Fu, Richard Zannoni, Fernando Rodriguez-Morales, John Nicholson, Stephan Adams, Chak Chan, Alexander de Geofroy, Eric Polizzi and Joerg Appenzeller

Abstract— **At the ISSTT2006, we presented experimental results for a new microwave (~ 1GHz) direct and heterodyne detector based on metallic Single-Walled Carbon Nanotubes (m-SWNTs). We now report on microwave detection in several different contact configurations, and the methods used to fabricate these. One such configuration is a log-periodic toothed terahertz antenna with which we have now (soon after the conference) detected terahertz radiation from laser sources up to 1.63 THz. We also report on *ab-initio* simulations relevant for interpreting the experimental data. We argue that exploring the properties of single m-SWNTs at terahertz should be very fruitful.**

I. Introduction

Single Wall Carbon Nanotubes (SWNTs) have been proposed for use of in many new types of electronic devices [1]. SWNTs can be either metallic or semiconducting [2]. One device that is being researched is the Carbon Nanotube Field Effect Transistor (CNT-FET) [3], [4] which employs semiconducting CNTs (s-SWNTs). Applications have also been proposed to detectors for microwave or terahertz frequencies. Schottky barriers exist at the contacts of semiconducting SWNTs [5], [6], and were fabricated and analyzed for use as terahertz detectors by Manohara *et al.* [7]. Experimental results were recently published by Rosenblatt *et al.* [8] demonstrating detection of microwaves up to 50 GHz, as well as by Pesetski *et al.* [9] who measured heterodyne detection with flat frequency-dependence up to 23 GHz. These references ([7]-[9]) all used the s-SWNT-FET configuration. Itkis et al. published results on a Near IR bolometric detector employing a CNT film in which it is likely that the metallic CNTs were most active. A similar bolometric CNT film detector was demonstrated at 94 GHz by Tarasov et al. [11]. Metallic SWNTs (m-SWNTs) have considerable potential for detector applications, and one of us (SY) recently proposed a very fast terahertz detector based on the hot electron bolometric (HEB) effect [12,13]. In the present paper we report experimental results for a device that uses an m-SWNT for detecting microwaves up to 12 GHz, as well as terahertz radiation up to 1.6 THz. In its microwave operation the device described here functions both as a direct (DC output) detector and as a heterodyne detector (difference frequency output up to at least 200 MHz). In this paper we will discuss the experimental results, the possible detection mechanisms involved, as well as relevant *ab-initio* simulations.

S. Yngvesson, K. Fu, R. Zannoni, J. Nicholson, S. Adams, A. de Geofroy, and E. Polizzi are with the Department of Electrical and Computer Engineering, University of Massachusetts, Amherst, MA 01003-9292.

F. Rodriguez-Morales was with the Department of Electrical and Computer Engineering, University of Massachusetts, Amherst, MA 01003-9292; he is now with the Center for Remote Sensing of Ice Sheets (CReSIS), University of Kansas, Lawrence, KS 66045.

C. Chan was with Holyoke Community College, Holyoke, MA; He is now with the Department of Electrical and Computer Engineering, University of Massachusetts, Amherst, MA 01003.

J. Appenzeller was with the IBM T.J. Watson Research Center, PO Box 2128, Yorktown Heights, NY 10598, USA. He is now with the Dept. of Electrical and Computer Engineering, Purdue University Birck Nanotechnology Center, West Lafayette, IN 47907-20575.

This work was supported by a grant for Nanoscale Exploratory Research from the National Science Foundation (ECS-0508436).

II. Experimental Methods and Results

A. Initial Experimental Procedures

SWNTs used in our study were grown using laser ablation [14]. They have diameters between 0.6 nm and 1.5 nm, and were contacted either at the IBM T.J. Watson Research Center, or at UMass/Amherst. In the IBM process they were spun from solution onto a p+-doped silicon substrate covered with 100 nm of silicon oxide. Contact strips of width 350 nm were made with 20 nm of Ti followed by 100 nm of Au, and were connected to 80 µm x 80 µm contact pads. The length of the tubes between contacts is known to be in the range of 300 nm to 500 nm.

In the UMass process, CNTs were also first spun onto doped silicon substrates. We used an available mask that produced long metal contact strips with different spacings from 4 to 8 µm and contact pads that could be wire-bonded.

In all subsequent microwave experiments the chip was placed in a small copper enclosure (with a metallic cover) to isolate it from external radiation, see Figure 1 for an example. The contact pads were connected by wire bonds to (1) a microstrip transmission line that was in turn connected to a standard coaxial connector installed in the side of the enclosure; and (2) the ground plane of the enclosure. The silicon substrate was left electrically insulated in order to minimize parasitic reactances. The assembly was placed in a liquid helium vacuum dewar and pumped to a good vacuum for at least one day in order to remove most of the surface contaminations on the CNT. A well shielded stainless steel coaxial cable makes the sample accessible from the outside of the dewar. We used a programmable DC power supply (Keithley) to provide a voltage source bias to the device through the coaxial cable. The DC supply measured the DC voltage and current, and these were read by a computer for further processing. Microwave sources (Agilent) were also fed to the coaxial cable, and different sources (DC and microwave) were separated through the use of commercial bias tees.

B. I-V-Curves and Microwave Detection

It is well-known that Ti/Au contacts yield a contact resistance that is usually quite high and strongly dependent on the nanotube diameter [15]-[17]. The devices used in our study had contact resistances that were in the range of a few hundred kΩ to a few MΩ. It is also known that the conductance of such

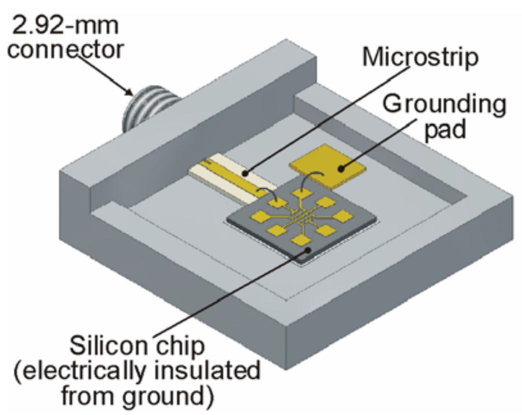

Figure 1. The experimental fixture used in this work.

CNTs shows a “zero-bias anomaly” [17-19], i.e. the differential conductance (dI/dV) plotted as a function of bias voltage (V) shows a dip at low values of V with a width of about +/- 400 mV. This presents a nonlinearity in the IV-curve (Figure 2; for an IBM device) that we exploited for microwave detection.

The zero-bias anomaly “dip” is also evident from the additional plot of dI/dV in Figure 2. This dip deepens as the temperature is decreased (the curves shown in Figure 2 were taken at 77K). At larger voltages the IV-curve shows a linear dependence between current and bias with a slight decrease in dI/dV for the highest voltage range. Except for the zero-bias anomaly, the IV-curve can thus be assumed to be due to a (roughly) constant contact resistance, that is weakly dependent on the temperature. Evidence from other metallic CNTs [4] indicates that the electrons have mean free paths of about 1μm; thus in our shortest tubes they travel ballistically from contact to contact. The zero-bias anomaly is usually ascribed to the very strong electron-electron Coulomb interactions in one-dimensional conductors that necessitates treating the electrons as a collective, plasmon-like, medium known as a “Luttinger liquid” (“LL”) [17]. Tunneling from the contacts into the LL is suppressed at low temperatures, which explains why the conductance approaches zero. It has been suggested that the behavior of the conductance in the entire temperature range from 4 K to 300 K can be better explained as being due to a combination of effects, the LL effect, and that of interfacial barriers at the contacts [18]. The LL effect is expected to be important only in the lowest temperature range.

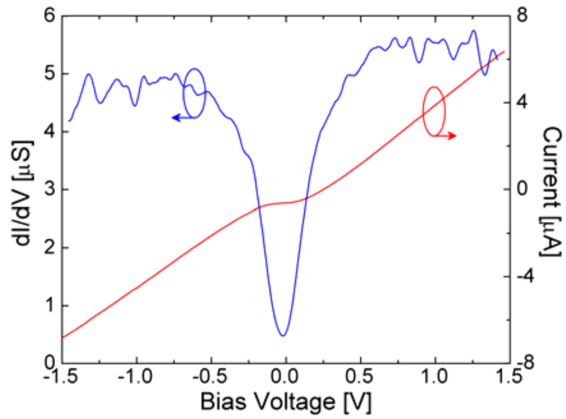

Figure 2. Measured IV-curve for a SWNT from IBM at 77 K (right scale); dI/dV based on the IV-curve (left scale).

As made clear in the paper mentioned above [18], a complete understanding of the contacts between the one-dimensional m-SWNTs and a 3-D metal is not yet available.

UMass devices with Ti/Au contacts were also fabricated with IV-curves similar to that in Figure 2. In a different process, we placed CNTs on top of Ti/Au contacts, and then added a further Pd contact metalization on top of the CNTs. This resulted in a much lower contact resistance, and an IV curve that was curved in the opposite direction, see Figure 3. The increased resistance at higher bias voltages is known to be due to optical phonon emission that requires a minimum electron energy of about 160 meV [4,19,20].

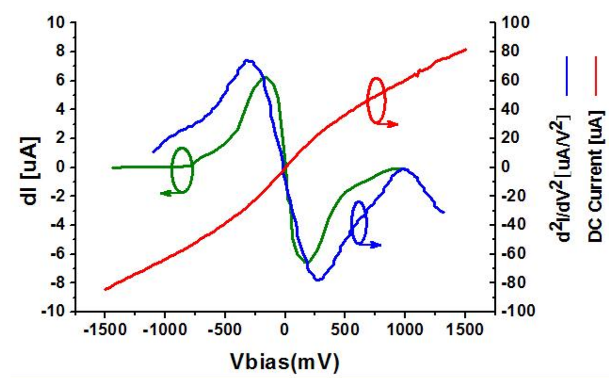

Figure 3. IV curve 77K (red) for CNT contacted with low resistance Pd contacts at UMass. The detected current change (ΔI) (green) is compared with d^2I/dV^2 (blue).

As microwaves were applied to the SWNT at 77K, we recorded a change in the device DC current (ΔI), and plotted this versus DC bias voltage (Figure 3). Similar recordings were also obtained for the IBM tubes, as reported earlier [21,22]. This recording was done by measuring the voltage across a series resistance with a lock-in amplifier, while square wave modulating the microwave source. The DC power supply was still configured as a voltage source. As shown in Figure 3, the detected current change varies with the bias voltage in the same way as d^2I/dV^2, the second-order derivative of the IV-curve. We can then interpret the detection process as a standard microwave detection process [23]. Theory and experiment agree quantitatively within 3dB. Heterodyne detection was demonstrated [21,22], and the microwave reflection coefficient (S11) was measured with an automatic network analyzer, as also reported in [21,22]. The detector response is flat to 900 MHz, and then falls off with the microwave frequency at about 12 dB per octave, consistent with a microwave model that was derived based on the S11 measurements. The modeling makes clear that the main factor that limits the frequency response is the very high doping of the silicon substrate used in all early measurements, as well as the large capacitance from the contact pads to the doped substrate.

C. Recent Experimental Procedures.

In order to explore the new detection process at higher frequencies we next fabricated devices on substrates that are insulating: sapphire and silicon-on-sapphire (SOS). Both of these substrates show good transmission up to high terahertz frequencies. New lithography masks were also designed and fabricated, with new contact configurations, see Figure 4: (1) Coplanar waveguides (CPW); and (2) Log-periodic toothed antennas, similar to designs we have previously used with NbN HEB mixers. The intention was to place CNTs across the narrow gaps at the center of these structures. The CPW mask has two parts, one for the center conductor and one for the outer conductors. These two parts of the mask can be adjusted in the lithography process resulting in different gap widths. The log periodic antenna has a gap of about 6 µm.

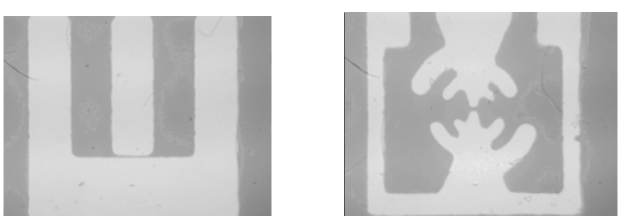

(a) **(b)**

Figure 4. Contact patterns for the new masks: (a) Coplanar waveguide; (b) Log-periodic antenna.

Each mask contains a large number of patterns of the types shown in Figure 4 (a) and (b) to maximize the probability of obtaining a CNT across the small gaps as they are spun on the substrates. The yield of tubes with acceptable IV-curves was found to be lower than when using contacts consisting of long, narrow strips, but several contacted tubes were found. The method of spinning the tubes onto the contacts in this case proved to result in unreliable contact performance, and few detection measurements were performed. The one shown in Figure 3 represents an exception, but in this case the contacts were improved by evaporating Pd on top of the CNTs.

Recently we have developed a much improved method for placing CNTs across the contacts, namely dielectrophoresis (DEP) [24-27]. In this method, an RF voltage (typically 5-10 V RMS, 5 MHz) is applied across a pair of electrodes, after a drop of a solution containing the CNTs is placed over the contacts. In our case, the CNTs were suspended in Isopropyl alcohol [25] and then ultra-sonicated for 10 minutes. The result of the DEP is that CNTs migrate in the solution toward the contacts, and then become attached to the contacts. It has also been observed that nearby contacts that experience a floating RF potential can attract CNTs [26]. The procedure typically takes only a few minutes. The DC resistance is being monitored as the DEP proceeds and the process is stopped when a desired IV-curve has been obtained. If a somewhat longer time is used a large number of CNTs will be collected on the contacts, with a typical minimum resistance of 500 Ω. In this case it is possible to gradually burn CNTs by using a higher voltage (DC or pulsed). We have implemented the DEP procedure for both contact patterns in Figure 4. One advantage is that the substrate need not contain many patterns, one is sufficient. Another advantage is that when the applied voltage has a frequency of 5 MHz or above metallic SWNTs are preferentially selected [24]. We assume that if a few s-SWNTs are also contacted in parallel with the m-SWNTs, their resistance is high enough that it can be neglected (no gate voltage is applied).

D. Recent Experimental Results – Microwave and Terahertz Detection

We have measured microwave detection in m-SWNTs placed by DEP and find similar results to the previous microwave experiments. One difference is that the detection persisted to higher frequencies, about 12 GHz. This was expected since we are now able to employ non-conducting substrates (sapphire and SOS) as mentioned above. A photograph of the fixture we use for the measurements is shown in Figure 5. This fixture was adapted from one previously used for NbN HEB mixers. The device chip in this case is SOS with dimensions 6 x 6 mm. Bond wires (3-4 mm long) are used to connect between a microstrip transmission line and the contact pads of the antenna. The bond wires have enough inductance to explain fall-off of the frequency response for microwave detection. The CPW structure has been tested in a microwave probe system, and this will be used to further extend the frequency response at microwave frequencies.

Figure 5. The fixture used for recent measurements of MW and terahertz detection in m-SWNTs. The device is biased through the SMA connector. The silicon lens located on the opposite side of the SOS substrate can be seen through this substrate.

A 4 mm diameter ellipsoidal silicon lens was attached with purified bees wax to the substrate for quasi-optical coupling to the antenna as discussed in [12,13]. Note that the dielectric constant of sapphire is a close match to that of silicon. The device was biased through a 100 kΩ sensing resistor that configured the Keithley supply as a voltage source. A lock-in amplifier was connected across that resistor in a balanced mode through two further 100 kΩ resistors in order to record the detected change in current through the device. The same fixture can then be used for both microwave and terahertz detection. Terahertz radiation was introduced through the silicon lens from a terahertz gas laser that has a typical output power of 2-5 mW. The laser was modulated at 1 kHz by inserting an acousto-optic modulator after the CO_2 pump laser. The modulator also provided the reference voltage for the lock-in amplifier.

Using this configuration we have now for the first time (soon after the conference) demonstrated detection at terahertz frequencies in a CNT. Three different frequencies were used (wavelength in μm is given in parenthesis): 0.694 THz (432); 1.04 THz (287); 1.63 THz (184); the IV-curve at 77 K is first displayed below in Figure 6.

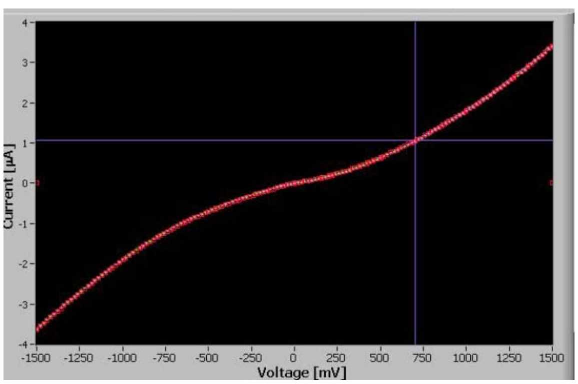

Figure 6. IV-curve for a device placed with DEP on the substrate shown in Figure 5.

The detected voltage on the lock-in amplifier is plotted versus the bias voltage in Figure 7 when the 432 μm line was used as input. The input power was 2.3 mW, measured on a Scientech power meter. The noise level was of the order of 4-5 μV, except for the highest bias voltages (near 1.5 V) where an increase in the 1/f noise from the CNT was evident. The S/N at the optimum bias point thus is about 25. These are preliminary data, but clearly show that the m-SWNT detects the terahertz radiation both at 300 K and at 77 K. Re-alignment of the laser produced slightly different responsivities, but all features were reproducible.

The highest frequency for which we obtained detection was 1.63 THz (184 μm), see Figure 8. We also attempted detection at 2.54 THz (118 μm) but were not successful so far. Two different (perpendicular) polarizations were employed, and it is not yet clear what the significance of the different responses for different polarizations is.

The bias voltage dependence of the detector response to terahertz radiation does not have a simple d^2I/dV^2 dependence, as it did for microwave detection (see Figure 3). We discuss different processes that may be responsible for the detection in section III. Much further work is clearly needed to identify the detection process(es) that actually occur(s). It is also noteworthy that the terahertz responsivity of the detector at this stage of the investigation is about the same at 300 K (~ 1.2 V/W) as it is at 77 K (2 V/W). The responsivities are uncorrected for the optical losses in the dewar window and the silicon lens (~3-4 dB). The same device has a microwave responsivity of 73 V/W at 300 K, a typical value for microwave responsivity. The largest microwave responsivity measured is 600 V/W, at 77 K, for the device with the IV-curve as given in Figure 3. Future work will also explore use of lower temperatures than 77 K, for which we earlier found a much larger responsivity at microwaves [12,13].

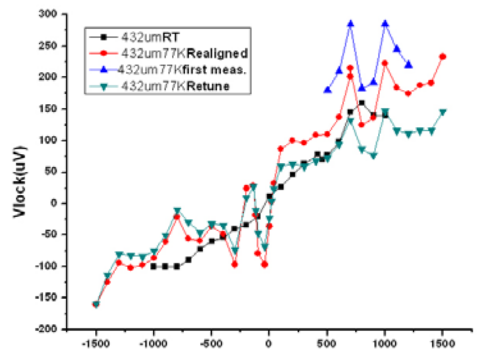

Figure 7. Detected voltage on the lock-in amplifier when the laser line at 432 μm was used.

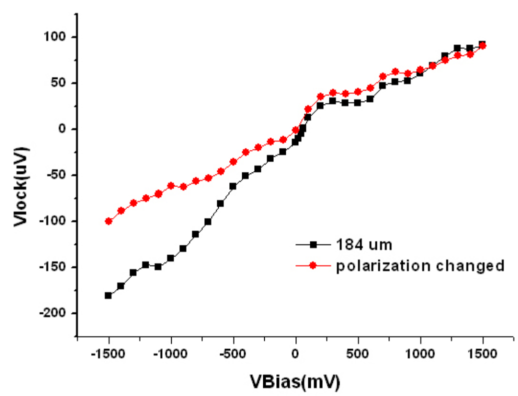

Figure 8. Detected voltage on the lock-in amplifier with an input frequency of 1.63 THz.

III. PREDICTED TERAHERTZ RESPONSE FOR M-SWNTS

A single m-SWNT can be modeled as shown below in Figure 9, based on the work of P.Burke and others [28]. The contents of the "cell" are meant to be repeated periodically. The periodically repeated cells model a transmission line with a propagation velocity of about 2.4 x 10^8 cm/s. The physical process this models is the plasmon mode we discussed in Sec. II.B. Based on this model one finds that the m-SWNT has a very large kinetic inductance (L_K), as well as a quantum capacitance (C_Q). The kinetic inductance of a single m-SWNT was recently measured with microwave network analyzer techniques, confirming a major aspect of the above model [29].

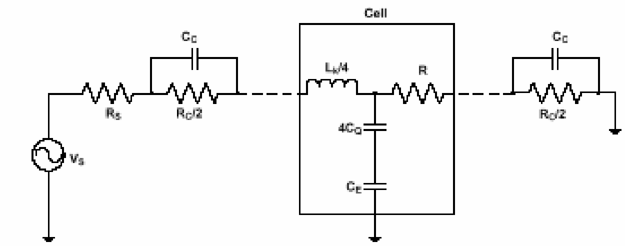

Figure 9. Circuit model for an m-SWNT.

The contact resistance (R_C) is typically large as also discussed in Sec. II.B, and often represents most of the measured DC resistance. R_C has a capacitance in parallel (C_C), however, and if C_C is large enough then R_C will be shunted and have a negligible effect at terahertz frequencies. We can then distinguish two types of cases:

CASE A (CNT nonlinearity): If the contact impedance is small, we see mainly the m-SWNT proper, and a reasonable fraction of the terahertz power will be absorbed in the tube, provided that its ohmic resistance is not too high.

CASE B (contact nonlinearity): In this case the contact resistance dominates the total impedance, as clearly occurs at microwave frequencies.

We have simulated the circuit in Figure 9 for CASE A and find the result shown in Figure 10. The m-SWNT was assumed to be 1 µm long and the plasmon wave shows a half-wave resonance at 1.2 THz. There is a second resonance at a much lower frequency due to a lumped circuit combination of the kinetic inductance and the contact capacitance.

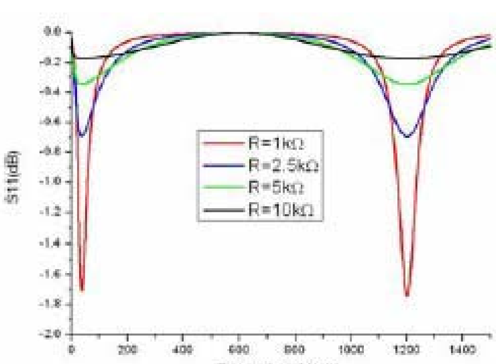

Figure 10. Simulated S11 response of a 1 µm long m-SWNT fed from a 100 Ω source (the LP antenna). Values assumed for the circuit in Figure 9 are $R_C/2 = 20$ kΩ, $C_C = 10$ fF, $L_K = 4$ nH [28], $C_E = 50$ aF [28] and $4C_Q = 400$ aF [28].

The CNT can be well matched to the antenna for the lower values of CNT resistance, which are expected to occur at lower temperatures. At room temperature the matching can be improved by designing a matching network, as shown in [13].

We have also simulated CASE B, and shown that excellent matching can be obtained at the lower terahertz frequencies. We can thus conclude that it is possible to efficiently absorb terahertz radiation in an m-SWNT. In CASE A we expect that the detection may occur due to HEB effects, as discussed earlier [11,12,21,22]. The responsivity will depend on the temperature dependence of the resistance, which can be quite substantial at the lower temperatures. CASE B has already been demonstrated at microwave frequencies, and further work will show to how high frequencies this process will be effective.

IV. AB INITIO SIMULATION OF METALLIC CARBON NANOTUBES

We have mentioned above that our theoretical understanding of m-SWNT properties such as contact resistance and capacitance, as well as transport properties, is quite limited at the present time. Reliable and accurate quantum simulations of CNTs are needed to clear up our understanding of many experimental issues and characterize our devices. These are being performed by the group of Professor Eric Polizzi.

In [30], we have achieved electron transport simulations of CNT-FETs based on Non-Equilibrium Green's Functions (NEGF). The results obtained have highlighted the huge influence of 3D electrostatics on the 1D CNT and the role of defects (vacancies and charged impurities) in altering nanotube transistor device characteristics from the ballistic transport limit.

In order to allow an accurate physical description of the contacts with the reservoirs, one needs to resort *to ab-initio* atomistic approaches such as density functional theory (DFT). For numerical reasons, *ab-initio* transport calculations are usually limited to isolated regions of the carbon nanotube close to the metal contacts or possible defects. An *ab-initio* atomistic description of the electron transport in the entire carbon nanotube, however, could provide important insights on electronic properties of the device while considering arbitrary length, chirality, diameters, etc. . . This type of "bottom-up" simulation is still a formidable task and we are making use of innovative numerical modeling strategies to realize this goal efficiently.

For *ab-initio* type calculations, as compared to other traditional methods, mesh techniques (such as the finite element method- FEM) present significant advantages which have been reviewed in [31]. For a 100 nm long CNT composed of ~10,000 atoms, one may typically obtain a Hamiltonian matrix size of 10^8. Within our real-space mesh framework, we have, however, been able to reduce the computational cost of the transport simulations by introducing novel strategies such as: sub-band decompositions, and preconditioning strategies for solving the resulting linear systems via iterative methods. We have then recently applied these techniques for *ab-initio* electronic structure calculations for a CNT. Our preliminary results are summarized in Figure 11. We also performed the calculation of the electron density.

In the future we plan to increase the level of sophistication of our model by introducing the following aspects:

1. A rigorous treatment of the CNT contacts.
2. A non-ballistic quantum transport model including phase-breaking dissipation processes (*e.g.*, electron-phonon scattering).
3. A time-dependent transport regime by adapting the transient simulation approach proposed in [32].

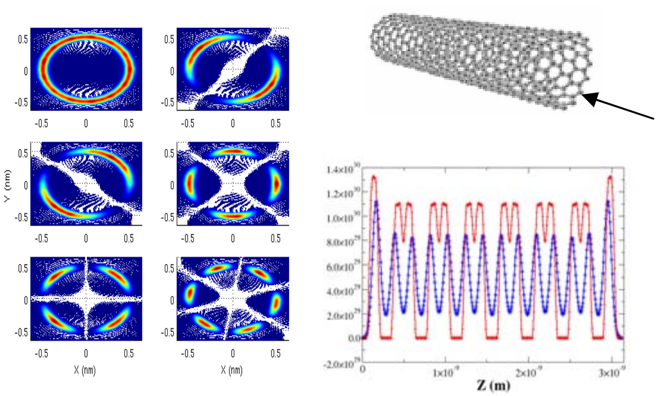

Figure 11. Preliminary results obtained using *ab-initio* electronic structure calculations of CNT and a real space mesh technique (FEM). On the left, the figures represent the first six modes at a given cross section of a (13,0) tube. On the right we choose to represent the variation of the electron density along the z direction starting from a given (x,y) atom node at the first cross section. The red cross curve is obtained using a semi-classical Thomas-Fermi approximation while the blue star curve represents the result of the quantum simulation. The length of the nanotube tube has been set at 3nm for the purpose of illustrating a simple case.

Ref. [32] studied non-quasi-static effects (NQSE) in CNT transistors. The NQSE are equivalent to the kinetic inductance (L_K) and quantum capacitance (C_Q) we introduced in Sec. III. This reference found that for CNT-FETs the intrinsic response can be accurately calculated *without* taking the NQSE into account, up to about 2 THz. One reason L_K can be neglected is that the fastest CNT-FETs are very short (~ 10nm). The difference in the present project is that we are experimentally studying configurations for which NQSE's are emphasized, and that measurements of such effects can be performed (see above), partly because parasitic effects have been minimized, which is not possible for CNT-FETs. Our continued *ab-initio* simulations will study in detail the device characteristic responses (I-V-curve, conductance, capacitance, inductance, etc…) to different excitations that may alter the terahertz experimental data such as defects, vacancies, charge impurities, and other distortions.

V. CONCLUSIONS

We have reported new results on microwave detection and the first detection of terahertz radiation in m-SWNTs. The path now lies open for further studies combining microwave and terahertz measurements with *ab-initio* simulations that explore the high-frequency properties of this unique medium.

REFERENCES

[1] P.L. McEuen, M. S. Fuhrer, and H. Park, IEEE Trans. Nanotechnol, **1**, 78 (2002).
[2] R. Saito, G. Dresselhaus, and M.S. Dresselhaus, *Physical Properties of Carbon Nanotubes* (Imperial College Press, London, 1998).
[3] Y.-M. Lin, J. Appenzeller, J. Knoch, and Ph. Avouris, IEEE Trans. Nanotechnol. **4**, 481 (2005).
[4] A. Javey, J. Guo, D.B. Farmer, Q. Wang, D. Wang, R.G. Gordon, M. Lundstrom, and H. Dai, Nano Lett. **4**, 447 (2004).
[5] S. Heinze, J, Tersoff, R. Martel, V. Derycke, J. Appenzeller, and Ph. Avouris, PRL **89**, 106801 (2002).
[6] J. Appenzeller, J. Knoch, V. Derycke, R. Martel, S. Wind, and Ph. Avouris, PRL **89**, 126801 (2002).
[7] H.M. Manohara, E.W. Wong, E. Schlecht, B.D. Hunt, and P.H. Siegel, Nano Lett. **5**, 1469 2005.
[8] S. Rosenblatt, H. Lin, V. Sazonova, S. Tiwari, and P.L. McEuen, Appl. Phys. Lett. **87**, 153111 (2005).
[9] A. A. Pesetski, J.E. Baumgardner, E. Folk, J. Przybysz, J. D. Adam, and H. Zhang, Appl. Phys. Lett., **88**, 113103 (2006).
[10] M.E. Itkis, F.Borondics, A.Yu, R.C. Haddon, Science **312**, 314 (2006).
[11] M. Tarasov, J. Svensson, L. Kuzmin, and E. E. B. Campbell, Appl.Phys.Lett., **90**, 163503 (2007).
[12] K.S. Yngvesson, Appl. Phys. Lett. **87**, 043503 (2005).
[13] K.S. Yngvesson, 16th Intern. Symp.Space Terahertz Technol., Gothenburg, Sweden, May 2005.
[14] A. Thess, R. Lee, P. Nikolaev, H. Dai, P. Petit, J. Robert, C. Xu, Y.H. Lee, S.G. Kim, A.G. Rinzler, D.T. Colbert, G.E. Scuseria, D. Tomanek, J.E. Fischer, and R.E. Smalley, Science **273,** 483 (1996).
[15] Z. Chen, J. Appenzeller, J. Knoch, Y.-M. Lin, and Ph. Avouris, Nano Lett. **5**, 1497 (2005).
[16] W. Kim, A. Javey, R. Tu, J. Cao, Q. Wang, and H. Dai, Appl. Phys. Lett. **87**, 173101 (2005).
[17] M. Bockrath, D.H. Cobden, J. Lu, A.G. Rinzler, R. E. Smalley, L. Balents and P. L. McEuen, Nature **397**, 598 (1999).
[18] Th. Hunger, B. Lengeler, and J. Appenzeller, Phys. Rev. B, **69**, 195406 (2004).
[19] Z. Yao, C.L. Kane, and C. Dekker, Phys. Rev. Lett. **84**, 2941 (2000).
[20] A. Javey, J. Guo, M. Paulsson, Q. Wang, D. Mann, M. Lundstrom, and H. Dai, Phys. Rev. Lett. **92**, 106804-1 (2004).
[21] K.S. Yngvesson, F. Rodriguez-Morales, R. Zannoni, J. Nicholson, M. Fischetti and J. Appenzeller, 17th Intern. Symp. Space Terahertz Technol., Paris, May 2006.
[22] F. Rodriguez-Morales, R. Zannoni, J. Nicholson, M. Fischetti, K. S. Yngvesson, and J. Appenzeller, Appl. Phys. Lett., **89**, 083502 (2006).
[23] K.S. Yngvesson, *Microwave Semiconductor Devices* (Kluwer Academic Publishers, Norwell, MA, 1991).
[24] R. Krupke and F. Hennrich, Adv. Engin. Materials, 7, 111 (2005).
[25] N. Peng, Q. Zhang, J. Li, and N. Liu, JAP **100**, 024309(2006).
[26] L. Dong et al., J.Phys.Chem. **109**,13148 (2005).
[27] Z-B. Zhang, X-J. Liu, E.E.B. Campbell, and S-L. Chang, JAP, **98**, 056103 (2005).
[28] P.J. Burke, IEEE Trans. Nano Technol. **1**, 129 (2002).
[29] J. J. Plombon, K. P. O'Brien, F. Gstrein, V. M. Dubin, and Y. Jiao, Appl. Phys. Lett., **90**, 063106 (2007).
[30] N. Neophytou, D. Kienle, E. Polizzi, M. P. Anantram, Appl. Phys. Lett. **88**, 242106 (2006).
[31] T. Beck, Rev. of Modern Phys., **72**, p1041, (2000).
[32] L. Latessa, A. Pecchia, and A. Di Carlo, IEEE Trans. Nanotechn, **6**, 13 (2007).